# On the Hydronium Ion Catalyzed Mechanism in Vinyl Alcohol−Acetaldehyde Isomerization: *Ab initio* Molecular Orbital Theory and Monte Carlo Simulation

**Masataka Nagaoka,* Katsuhiro Suenobu,† and Tokio Yamabe‡**

*Contribution from the Institute for Fundamental Chemistry, 34-4, Takano-Nishihiraki-cho, Sakyo-ku, Kyoto 606, Japan, and Department of Molecular Engineering, Kyoto University, Sakyo-ku, Kyoto 606, Japan*

*Received November 18, 1996. Revised Manuscript Received June 2, 1997*[⊗]

**Abstract:** The hydronium ion catalyzed vinyl alcohol−acetaldehyde isomerization was investigated via *ab initio* molecular orbital (MO) calculations with/without a dielectric continuum (DC) method and Monte Carlo (MC) simulations with the statistical perturbation theory. The cluster models, composed of $CH_2$═CHOH, $H_3O^+$, and $H_2O$ molecules, were considered, and the potential energy profiles of double proton transfers both in the gas phase and in the aqueous solution were obtained by *ab initio* MO calculations. In order to clarify the mechanism suitable for the reaction, two possible mechanisms, concerted and stepwise, have been proposed. Our results indicated that the double-proton transfers prefer to occur separately not only in the gas phase but also in the aqueous solution, to support the preference for the stepwise mechanism. The solvent effect difference between the DC method and MC simulations was also examined along the stepwise reaction path by plotting the free energy profiles. It was found that MC simulations improve considerably the energy barrier of activation by the DC method (5.0 kcal/mol) to present 13.5 kcal/mol for the free energy barrier of activation. The present value shows good accordance with the experimental value, i.e., 15.2 kcal/mol.

## I. Introduction

In not only organic chemistry but also biochemistry,[1] tautomerism is one of the most important and valuable research subjects from both experimental and theoretical points of view. In particular, the most typical tautomerism of the keto−enol isomerization has been studied extensively both experimentally and theoretically.[1,2] For many years, it has been conventionally a chemical common sense that vinyl alcohol (VA), the simplest enol, should be classified as extremely unstable,[1,2] and therefore, some chemists still might not believe in its existence. However, since the slow tautomerization of VA to acetaldehyde (AA) has been reported by Capon *et al*., who investigated the acid-catalyzed hydrolysis of vinyl orthoesters at low temperature, it has been regarded as a chemical fact that the species should be quite stable under some appropriate conditions and could be readily synthesized and observable.[1,2] Thereafter, the VA−AA rearrangement has been a revival of a topic for theoretical and experimental investigations.[1−8]

On the other hand, in the field of polymer synthesis, Novak *et al.* have reported that, through preparation of O−D vinyl alcohol using only slightly more than a stoichiometric amount of water, the half-life of VA could be extended from 10 min to many hours at room temperature. With these conditions, VA can now be thought of as a useful substrate to synthesize poly(vinyl alcohol) (PVA) directly.[9] In appropriate conditions, VA could be polymerized faster than the competing tautomerization process.

Under the recent circumstances, estimation of the rates of interconversion of VA to AA and the reverse reaction is crucially important to discriminate whether such a new synthetic scheme would become realizable or not. Therefore, in this paper, we have investigated the reaction mechanism of conversion between VA and AA and exposed its free energy profile by theoretical methods using *ab initio* molecular orbital (MO) theory and Monte Carlo (MC) calculations. Experimentally, those rates of interconversion between VA and AA, have been measured, so far, in aqueous solution, having provided thermodynamic parameters such as equilibrium constants, to propose several possible reaction mechanisms.[1,6,7] In particular, the reaction mechanism of the hydronium ion catalyzed ketonization has become a focus of attention because two possible mechanisms were considered, as shown in Figure 1. Capon *et al.* proposed the concerted mechanism where the protonation of $\beta$-carbon of VA and the proton removal from its hydroxyl group occur simultaneously.[6] Their conclusions were based on arguments for the reactivity comparison between the ketonization of VA and the vinyl ether hydrolysis.[1,6] Vinyl ether hydrolysis is believed to occur by the rate-determining proton transfer from a catalyzing acid to vinyl carbon,[10] which is a characteristic in common with enol ketonization. A concerted mechanism for vinyl ether hydrolysis is improbable because simultaneous loss of alkyl group is unlikely to occur.[11] There should then be a close correspondence between vinyl ether hydrolysis and ketonization if the latter occurs by a stepwise mechanism. On the other hand, if the concerted mechanism is probable for ketonization, there should be some predictable differences between these two reactions. For example, Capon *et al.* pointed

* Author to whom correspondence should be addressed.
† Permanent address: Organic Synthesis Research Laboratory, Sumitomo Chemical Co., Ltd., 10-1, 2-Chome, Tsukahara, Takatsuki-City, Osaka 569, Japan.
‡ Kyoto University.
⊗ Abstract published in *Advance ACS Abstracts,* August 1, 1997.
(1) *The Chemistry of Enols*; Rappoport, Z., Ed.; Wiley: New York, 1990.
(2) Capon, B.; Guo, B.; Kwok, F. C.; Siddhanta, A. K.; Zucco, C. *Acc. Chem. Res.* **1988**, *21*, 135.
(3) Smith, B. J.; Nguyen, M. T.; Bouma, W. J.; Radom, L. *J. Am. Chem. Soc.* **1991**, *113*, 6452.
(4) Ventura, O. N.; Lledos, A.; Bonaccorsi, R.; Bertran, J.; Tomasi, J. *Theor. Chim. Acta.* **1987**, *72*, 175.
(5) Poirier, R. A.; Yu, D.; Surjan, P. R. *Can. J. Chem.* **1991**, *69*, 1589.
(6) Capon, B.; Zucco, C. *J. Am. Chem. Soc.* **1982**, *104*, 7567.
(7) Chiang, Y.; Hojatti, M.; Keefe, J. R.; Kresge, A. J.; Schepp, N. P.; Wirz, J. *J. Am. Chem. Soc.* **1987**, *109*, 4000.
(8) Bouma, W. J.; Radom, L. *J. Mol. Struct.* **1978**, *43*, 267.
(9) Cederstav, A. K.; Novak, B. M. *J. Am. Chem. Soc.* **1994**, *116*, 4073.
(10) Kresge, A. J. *Acc. Chem. Res.* **1987**, *20*, 364.

S0002-7863(96)03994-7 CCC: $14.00 

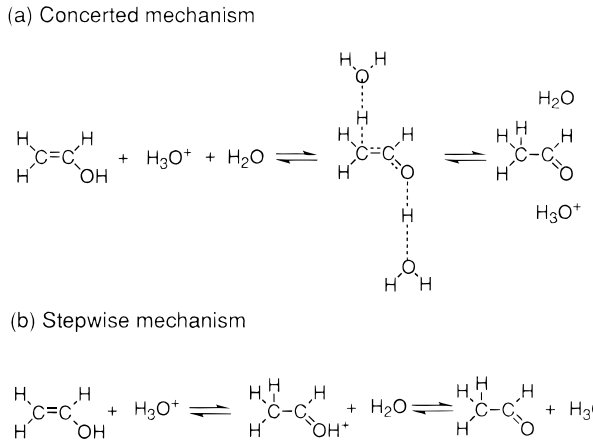


**Figure 1.** Two mechanisms of the hydronium ion catalyzed ketonization of vinyl alcohol: (a) concerted mechanism and (b) stepwise mechanism.

out that the large differences found in the change of rate constants following to the change of solvent constitution could be explained by the concerted mechanism.[6]

Chiang *et al.* proposed the stepwise mechanism rather than the concerted one from experimental results of kinetic solvent isotope effects on both enolization and ketonization.[7] In the stepwise mechanism, the $\beta$-carbon of VA is protonated by hydronium ion in the first step and its hydroxyl group is deprotonated by solvent water in the second step.[7] They calculated the ratio of the rate constant of enolization in $H_2O$ to that in $D_2O$ ($k_{H2O}/k_{D2O}$) for both the concerted and the stepwise mechanism with fractionation factor theory[12] and compared it with the experimental value. As a result, the calculated value for the stepwise mechanism was close to the experimental one. Furthermore, Keeffe *et al.* discussed this more extensively and concluded that the arguments used by Capon *et al.* to support the concerted mechanism are not compelling.[1] They showed that the differences in solvent isotope effects and the medium effects for enol ketonization and vinyl ether hydrolysis do not require a concerted mechanism.

Theoretical investigations concerned with this isomerization have also been extensively reported.[1,3−5] For example, Smith *et al.* examined the potential energy surface (PES) of $C_2H_4O$ by *ab initio* MO theory to explain the isomerization of this system observed experimentally in the gas phase.[3] They revealed that VA is less stable by 11.2 kcal/mol than AA and has a barrier of 56.2 kcal/mol for ketonization at the G1 level of theory.[13] Ventura *et al.* examined the potential energy surface of ketonization of VA in aqueous solution by *ab initio* MO calculations with a dielectric continuum (DC) model (the SCRF method).[4] Although their aim was to reveal the most favorable mechanism among three possible ones for the water catalyzed ketonization of VA, it was concluded that three possible mechanisms are almost equally probable. To our knowledge, however, no theoretical investigation has been reported with respect to the suitable mechanism of the hydronium ion catalyzed reaction.

Under the circumstances, to understand the most suitable mechanism of the VA−AA tautomerization from the theoretical viewpoint, we report our investigation via *ab initio* MO theory and MC simulations by using the cluster models. The cluster includes a hydronium ion, a water, and a VA molecule. PESs

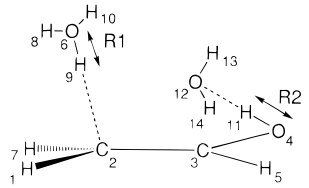


**Figure 2.** The cluster model composed of three molecules, $H_3O^+$, $H_2O$, and $CH_2$═CHOH. R1 and R2 represents the distance between O6 and H9 and that between O4 and H11, respectively.

for the double proton transfer reactions in the gas phase and the aqueous solution were obtained by *ab initio* MO calculations with/without the self-consistent reaction field (SCRF) method,[14] and their validity was examined. In addition, MC simulations with the statistical perturbation theory[15] were executed as well to obtain quantitatively the difference in free energy of solvation for the stepwise reaction path that would be found more probable.

Section II explains the present theoretical model on the basis of *ab initio* MO theory and MC treatment. In section III, results and discussion are made. Finally, the conclusions are drawn in section IV.

## II. Method of Calculation

**A. *Ab Initio* MO Calculations.** Since the direct *ab initio* MO calculation for the whole solution system is still unrealistic, we considered a cluster model taking the SCRF method[14] into account at the same time. The cluster model is composed of three molecules, $H_3O^+$, $H_2O$, and $CH_2$═CHOH, as shown in Figure 2. According to the proposed mechanisms,[6,7] it can deal with two proton transfers in the reaction, one of H9 from O6 to C2 and the other of H11 from O4 to O12. VA is assumed to hold the *s-cis* conformation throughout the reaction since there are experimental and theoretical evidences that the *s-cis* conformation is more stable than the *s-trans* conformation.[2,8]

Denoting the interatomic distance between atoms A and B as $R$(A−B), $R$(O6−C2) and $R$(O4−O12) are fixed as constant on the assumption that these heavy atoms should not move drastically during the proton transfer reaction, under the constraint by those surrounding solvent molecules in the aqueous solution. These two distances were determined separately by considering the structures of such complexes as $(H_2O)_2H_3O^+\cdots CH_2$═CHOH, $CH_3CHOH^+\cdots H_2O$, and $CH_2$═$CHOH^+\cdots H_2O$, which should be important as partial structures for the ketonization reaction of vinyl alcohol as shown in Figure 3. These structures were fully optimized by the HF/6-31G* method.

In the process to define $R$(O6−C2), although we expected at first some binding complexes of $H_3O^+\cdots CH_2$═CHOH, it was found that the $\beta$-carbon of vinyl alcohol was protonated by the hydronium ion without potential energy barrier, and hence, no stable complex exists. Therefore, $(H_2O)_2H_3O^+$ was used instead of $H_3O^+$ for including the charge delocalization effect, and we then obtained a stable complex such as $(H_2O)_2H_3O^+\cdots CH_2$═CHOH with $R$(O6−C2) = 3.07 Å (Figure 3a).

For $R$(O4−O12), two values, i.e., 2.91 and 2.60 Å, are assumed presently, reflecting the structures for the $CH_2$═$CHOH\cdots H_2O$ and the $CH_3CHOH^+\cdots H_2O$ complexes. The former complex represents the couple of a VA molecule and a solvent water molecule as a proton acceptor as a whole and corresponds to a partial model of the initial structure for the reaction. However, the latter represents the couple of a protonated VA and a solvent water molecule, corresponding to a model of the intermediate in the stepwise mechanism. Considering both the values of $R$(O6−C2) and $R$(O4−O12), two cluster models were constructed, referred to as Case I ($R$(O6−C2) = 3.07 Å, $R$(O4−O12) = 2.91 Å) and Case II ($R$(O6−C2) = 3.07 Å, $R$(O4−O12) = 2.60 Å) hereafter. As will be discussed in section III, since Case II would give a better potential energy profiles, it was also considered.

(11) Kiprianova, L. A.; Rekasheva, A. F. *Dokl. Akad. Nauk SSSR* **1962**, *142*, 589.
(12) Kresge, A. J. *Pure Appl. Chem.* **1964**, *8*, 243.
(13) Pople, J. A.; Head-Gordon, M.; Fox, D. J.; Raghavachari, K.; Curtiss, L. A. *J. Chem. Phys.* **1989**, *90*, 5622.
(14) Wong, M. W.; Frisch, M. J.; Wiberg, K. B. *J. Am. Chem. Soc.* **1991**, *113*, 4776.
(15) Zwanzig, R. W. *J. Chem. Phys.* **1954**, *22*, 1420.

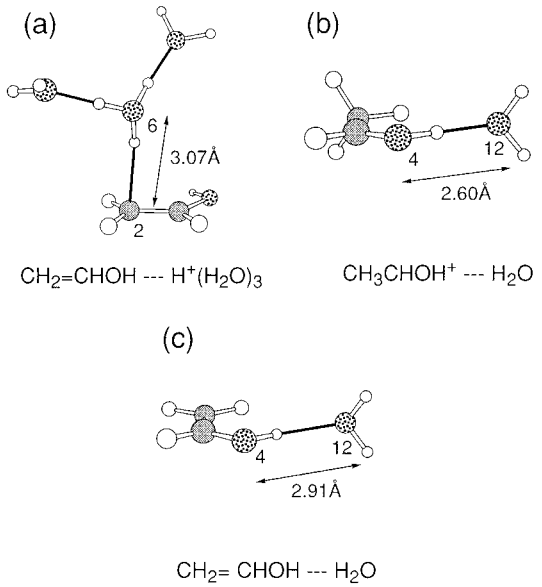


**Figure 3.** The optimized structures of three types of complexes for determining the interatomic distances *R*(O2-O6) and *R*(O4−O12): (a) the complex for *R*(C2-O6) in Cases I and II, (b) that for *R*(O4−O12) in Case I, and (c) that for *R*(O4−O12) in Case II.

Thus, 2.91 and 2.60 Å were adopted respectively for two values for *R*(O4−O12), corresponding to the above two complexes.

For the cluster models in the gas phase, we have prepared the two-dimensional potential energy profiles (i.e., contour plots), each as a function of two variables *R*(O6−H9) and *R*(O4−H11) which are denoted R1 and R2 in Figure 2. The potential energies have been calculated successively, for Case I, by changing R1 from 0.9 to 2.1 Å and R2 from 0.9 to 2.0 Å at intervals of 0.1 Å step and similarly, for Case II, by changing R1 from 0.9 to 2.1 Å and R2 from 0.9 to 1.7 Å. The total number of the points for which the potential energy was calculated were 156 for Case I and 117 for Case II. For optimization at each step, two geometry constraints were considered. First, the dihedral angle $\phi$(C2−C3−O4−O12) was fixed to be 0°. This constraint was necessary for holding the structure where the double-proton transfers could occur, modeling the reaction mechanism in aqueous solution. Second, the atoms, O6, H9, and C2, are always aligned linearly, as are the atoms O4, H11, and O12.

Geometry optimizations were done with the HF/6-31G* level and the three minima and two transition states were obtained. For all of the stationary points, geometry optimizations with the MP2/6-31+G** level were executed to examine the electron correlation effect. In this case, we fixed ∠C3−C2−O6 to that obtained from the HF/6-31G* level to model the reaction path. To consider the solvent effect for the cluster model, the SCRF method[14] implemented in the GAUSSIAN 94 program[16] was utilized at the same time. In the SCRF formalism, the solute is placed in a spherical cavity immersed in a continuous medium with a dielectric constant $\epsilon$. A dipole in the solute induces a dipole in the medium, and the electric field applied to the solute by the solvent dipole in turn interacts with the solute dipole to result in stabilization. A Born charge term[17] is also added to the expression of energy to include the ion−dipole interaction. Using the optimized geometries for the gas phase calculations of the cluster, we have determined the cavity radii by the method implemented in the GAUSSIAN 92,[18] and then have performed successive single-point calculations by introducing the bulk water influence within the DC approximation. The dielectric constant $\epsilon$ was assumed to be 78.5 for the bulk water. As a result, we have obtained two PESs for Cases I and II in the aqueous solution as well as in the gas phase. All calculations were done at the HF/SCRF/6-31G* level. Single-point calculations were also done with the MP2/SCRF/6-31+G** level using the MP2/6-31+G**-optimized geometries for considering the electron correlation effect.

**B. Monte Carlo Simulation.** For the reaction path obtained by *ab initio* MO calculations of the cluster models, Monte Carlo calculations with the statistical perturbation theory[15] were applied to calculate quantitatively the differences in free energy of solvation, to compare not only with the SCRF results but also with the experimental estimate. In the present model, the clusters were regarded as solutes and were placed in a cubic box (25 Å for each side), surrounded by 508 solvent water molecules. Monte Carlo simulations were executed in the NPT ensemble at 25 °C and 1 atm with Metropolis sampling and periodic boundary conditions. The system was perturbed between adjacent structural points *i* and *j*, and the free energy differences $\Delta G_{ij}$ were calculated as follows

$$\Delta G_{ij} = G_j - G_i = -kT \ln\langle \exp(-(E_j - E_i)/kT)\rangle_i \qquad (1)$$

where $E_i$ is the total energy of the point *i*, *k* is the Boltzman constant, and *T* is the absolute temperature. Each simulation involved $10^6$ configurations of equilibration and $2 \times 10^6$ configuration of averaging. All of the simulations were executed using the BOSS program.[19]

The intermolecular interactions were described by potential functions consisting of Coulomb and Lennard−Jones (LJ) terms between the atom *i* in the molecule *a* and the atom *j* in the molecule *b*, which are separated by a distance $r_{ij}$ as shown in eq 2.

$$\Delta E_{ab} = \sum_i \sum_j \{q_i q_j e^2/r_{ij} + 4\epsilon_{ij}[(\sigma_{ij}/r_{ij})^{12} - (\sigma_{ij}/r_{ij})^6]\} \qquad (2)$$

The TIP4P model[20] was used for the solvent water. For the solute, the CHELPG charges[21] with the HF/6-31G* method were calculated for each system and were assigned to all atoms in the solute as partial charges $q_i$ and standard united atom LJ parameters were adopted with geometric combining rules.[22]

$$\epsilon_{ij} = (\epsilon_i \epsilon_j)^{1/2} \qquad \sigma_{ij} = (\sigma_i \sigma_j)^{1/2} \qquad (2)$$

LJ parameters for the $\beta$-carbon of vinyl alcohol were taken from the OPLS parameters for alkene[23] and acetone[24] and were linearly scaled as the proton transfer proceeds. Similarly, those for the α-carbon and oxygen were from alcohol[25] and acetone.[24] Those for hydronium oxygen and water oxygen in the cluster are adopted from the TIP4P water model, and the values were not changed throughout the reaction.

## III. Results and Discussion

**A. Case I (*R*(O4−O12) = 2.91 Å).** Figure 4 shows the contour plot of the two-dimensional PES with the HF/6-31G* method for Case I in the gas phase. We have found three energy minima for three stable structures of the cluster at (R1, R2) = (1.0, 1.0), (2.0, 1.0), and (2.0, 1.9), denoted as A, B, and C,

(16) *Gaussian 94*, Revision A.1; Frisch, M. J.; Trucks, G. W.; Schlegel, H. B.; Gill, P. M. W.; Johnson, B. G.; Robb, M. A.; Cheeseman, J. R.; Keith, T. A.; Petersson, G. A.; Montgomery, J. A.; Raghavachari, K.; Al-Laham, M. A.; Zakrzewski, V. G.; Ortiz, J. V.; Foresman, J. B.; Cioslowski, J.; Stefanov, B. B.; Nanayakkara, A.; Challacombe, M.; Peng, C. Y.; Ayala, P. Y.; Chen, W.; Wong, M. W.; Andres, J. L.; Replogle, E. S.; Gomperts, R.; Martin, R. L.; Fox, D. J.; Binkley, J. S.; Defrees, D. J.; Baker, J.; Stewart, J. P.; Head-Gordon, M.; Gonzalez, C.; Pople, J. A.; Gaussian, Inc.: Pittsburgh, PA, 1995.

(17) Born, M. *Z. Phys.* **1920**, *1*, 45.

(18) *Gaussian 92*, Revision A; Frisch, M. J.; Trucks, G. W.; Head-Gordon, M.; Gill, P. M. W.; Wong, M. W.; Foresman, J. B.; Johnson, B. G.; Schlegel, H. B.; Robb, M. A.; Replogle, E. S.; Gomperts, R.; Andres, J. L.; Raghavachari, K.; Binkley, J. S.; Gonzalez, C.; Martin, R. L.; Fox, D. J.; Defrees, D. J.; Baker, J.; Stewart, J. J. P.; Pople, J. A.; Gaussian, Inc.: Pittsburgh, PA, 1992.

(19) Jorgensen, W. L. *BOSS*, Version 3.6; Yale University, New Haven, CT, 1995.

(20) Jorgensen, W. L.; Chandrasekhar, J.; Madura, J. D.; Impey, R. W.; Klein, M. L. *J. Chem. Phys.* **1983**, *79*, 926.

(21) Breneman, C. M.; Wiberg, K. B. *J. Comput. Chem.* **1990**, *11*, 361.

(22) Duffy, E. M.; Severance, D. L.; Jorgensen, W. L. *J. Am. Chem. Soc.* **1992**, *114*, 7535.

(23) Jorgensen, W. L.; Madura, J. D.; Swenson, C. J. *J. Am. Chem. Soc.* **1984**, *106*, 6638.

(24) Jorgensen, W. L.; Briggs, J. M.; Contreras, M. L. *J. Phys. Chem.* **1990**, *94*, 1683.

(25) Jorgensen, W. L. *J. Phys. Chem.* **1986**, *90*, 1276.

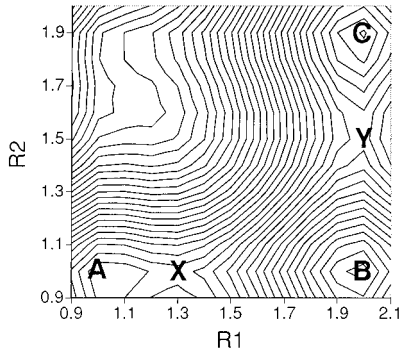


**Figure 4.** The contour plot of the potential energy surface for Case I in the gas phase (HF/6-31G*). Contour lines are plotted at 2.5 kcal/mol intervals.

respectively, where the unit of R1 and R2 is angstroms. A and B are separated by a transition state X at (R1, R2) = (1.3, 1.0), and B and C are separated by a transition state Y at (R1, R2) = (2.0, 1.5). Figure 5 shows the optimized structures obtained for A, X, B, Y, and C. The process A → X → B corresponds to the proton transfer from the hydronium ion to the $\beta$-carbon of vinyl alcohol and has a barrier of 3.6 kcal/mol. In this process, the change of hybridization (from $sp^2$ to $sp^3$) is clearly found for the $\beta$-carbon of vinyl alcohol as shown in Figure 5. The process B → Y → C corresponds to the proton transfer from the hydroxyl group of protonated vinyl alcohol to the solvent water molecule with a 30.0 kcal/mol barrier. These two processes constitute the stepwise ketonization of vinyl alcohol. However, any transition state for the concerted process does not exist in the PES. Thus, the stepwise proton transfer is favorable for Case I in the gas phase.

In Figure 6, the contour plot of the PES with the HF/SCRF/6-31G* method for Case I in the aqueous solution is shown. The geometrical structures of A, X, B, Y and C in Figure 6 are identical with those in Figure 4, and these points still correspond to the stationary points. The barriers of A → X → B and B → Y → C become 8.8 and 27.1 kcal/mol, respectively, and show considerable deviation from those values in the gas phase. However, by comparing the topologies of the two contour plots (Figures 4 and 6), one can understand that the present solvent effect is not so large that it might change the reaction mechanism from the stepwise proton transfer to the concerted one.

The relative energy diagram by the HF/6-31G* method is drawn in Figure 7 for the points, A, X, B, Y, and C, in both the gas phase and the aqueous solution. In both phases, B is the most stable among all stationary structures. The barrier height of the process A → X → B is 5.2 kcal/mol larger in the aqueous solution than in the gas phase and that of the process B → Y → C is inversely 2.9 kcal/mol smaller than in the gas phase. This characteristic comes from the dipole moment differences among A, X, B, Y, and C, whose dipole moments are 7.8, 5.2, 0.7, 4.5, and 8.5 D, respectively. Point A is stabilized more by the reaction field than point X, and point B is stabilized less than point Y.

For the purpose of knowing the electron correlation effect, the relative energy diagram with the MP2/6-31+G** method is shown in Figure 8 for Case I. By comparing it with that by the HF/6-31G* method (Figure 7), one notices two characteristics. First, although intermediate B is still the most stable among all states both in the gas phase and in the aqueous solution, it is found that the relative stability becomes smaller: Namely, the energy difference between A and B for Case I in the aqueous phase, for example, decreased from 27.0 kcal/mol (the HF/6-31G* method) to 17.9 kcal/mol (the MP2/6-31+G** method). Second, the two barrier heights for A → X → B and B → Y → C became lower and then became 6.9 and 18.4 kcal/mol in aqueous solution, respectively, in contrast with the values without the electron correlation, i.e., 8.8 and 27.1 kcal/mol.

**B. Case II ($R$(O4−O12) = 2.60 Å).** On the other hand, Figure 9 shows the contour plot of PES with the HF/6-31G* method for Case II in the gas phase. Similarly to Case I, three energy minima, D, E, and F, are obtained at (R1, R2) = (1.0, 1.0), (2.0, 1.0), and (2.0, 1.5), and two transition states, P and Q, are obtained at (R1, R2) = (1.3, 1.0) and (2.0, 1.4), respectively. Figure 10 shows the optimized structures obtained for D, P, E, Q, and F. The barriers for D → P → E and E → Q → F are each 2.7 and 14.2 kcal/mol, respectively. From the PES, it is found that the stepwise proton transfer is favorable for Case II in the gas phase.

In Figure 11, the contour plot of the PES with the HF/SCRF/6-31G* method is shown for Case II in the aqueous solution. The points Q′ and F′ are slightly different from those points (Q and F) on the PES in the gas phase, namely, the value of R2 for Q′ is 0.1 Å smaller than that for Q (R2 = 1.4) and the value of R2 for F′ is 0.1 Å larger than that for F (R1 = 1.5). The barriers of D → P → E and E → Q′ → F′ become 8.0 and 10.4 kcal/mol, respectively. As shown in Figure 12, the barrier height of the process D → P → E is 5.3 kcal/mol larger in the aqueous solution than in the gas phase, and that of the process E → Q′ → F′ is inversely 3.8 kcal/mol smaller than in the gas phase. This characteristic, similar to that in Case I, also comes from the dipole moment differences among D, P, E, Q′, and F′, whose dipole moments are 7.8, 5.1, 1.3, 3.9, and 7.0 D, respectively. By comparing the topologies of the two contour plots (Figures 9 and 11), we concluded that the stepwise mechanism is also favorable for Case II.

The relative energy diagram with the MP2/6-31+G** method is shown in Figures 13 for Case II. By comparing it with that by the HF/6-31G* method (Figure 12), one can notice two characteristics similar to those for Case I discussed above: Namely, the relative stability of the intermediate E becomes smaller and the two barrier heights for D → P → E and E → Q(Q′) → F(F′) become lower. By comparing the relative energy diagram for Case II with the MP2/6-31+G** method (Figure 13) with that of Case I (Figure 8), we can understand that the barrier height of the second proton transfer E → Q(Q′) → F(F′) becomes much lower than that of Case I due to the shorter $R$(O4−O12). Therefore, it is concluded that, to promote efficiently the present proton transfer reaction, the distance $R$(O4−O12) should be comparatively as short as 2.61 Å, which could be realized in the real experimental condition by the number of surrounding water molecules around O4 and O12.

**C. Monte Carlo Simulations.** We now understood the preference of the shorter $R$(O4−O12) by the cluster models. Furthermore, to reproduce theoretically the experimental prediction better than that in the cluster models, the statistical perturbation theory was applied for the reaction path D → P → E and E → Q → F for Case II. Figure 14 shows the change in free energy of solvation along with the reaction path D → P → E. It increases rapidly until R1 becomes 1.5 Å and then stays almost constant. The difference in free energy of solvation between D and P is 12.7 ± 0.5 kcal/mol, and this indicates that the transition state P is destabilized by hydration compared with D and is consistent with the SCRF results.

Figure 15 shows the change in free energy of solvation along with the reaction path E → Q → F. It decreases monotonically as R2 increases. The difference in free energy of solvation between E and Q is −6.4 ± 0.3 kcal/mol, and this indicates that the transition state Q is stabilized more by solvation than E and is also consistent with the SCRF results. The comparison

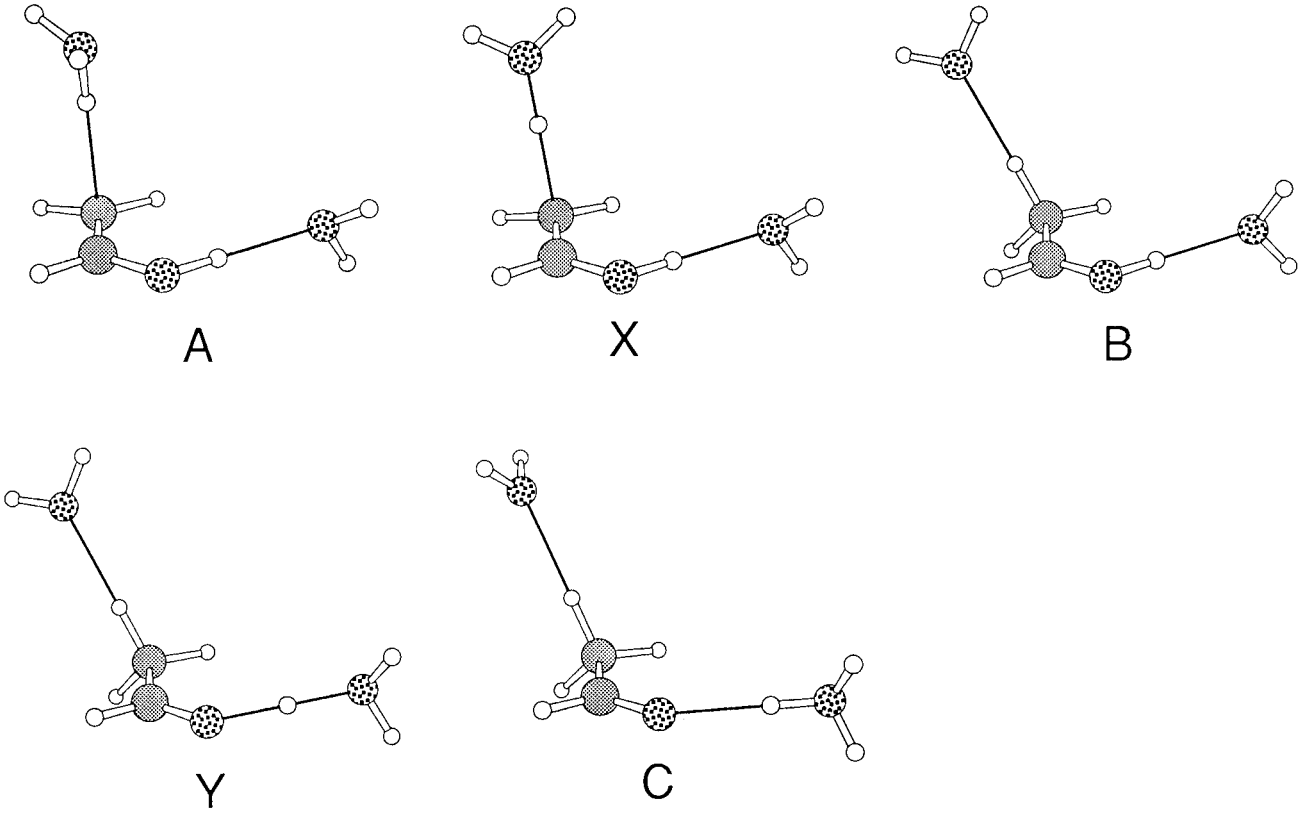


**Figure 5.** The optimized structures for the stationary points, A, X, B, Y, and C, respectively.

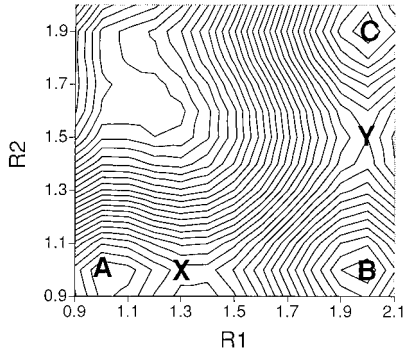


**Figure 6.** The contour plot of the potential energy surface for Case I in the aqueous solution (HF/SCRF/6-31G*). Contour lines are plotted at 2.5 kcal/mol intervals.

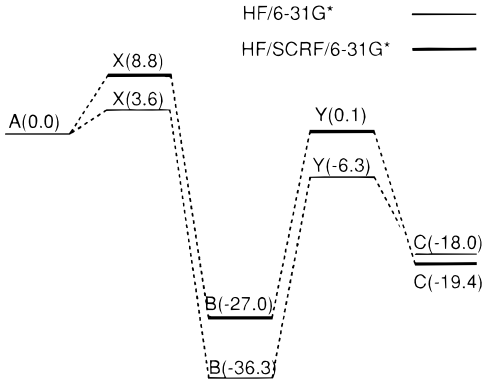


**Figure 7.** Relative energy diagram of Case I with the HF/6-31G* method in the gas phase (HF/6-31G*) and the aqueous solution (HF/SCRF/6-31G*). Numerical values are given in kcal/mol.

between the SCRF energy profile and Monte Carlo results is made for D → P → E in Figure 16 and E → Q → F in Figure 17. The free energy changes along the reaction paths are defined

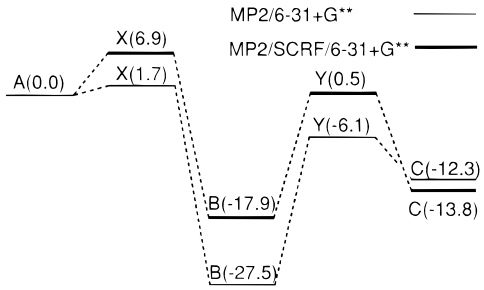


**Figure 8.** Relative energy diagram of Case I with the MP2/6-31+G** method in the gas phase (MP2/6-31+G**) and the aqueous solution (MP2/SCRF/6-31+G**). Numerical values are given in kcal/mol.

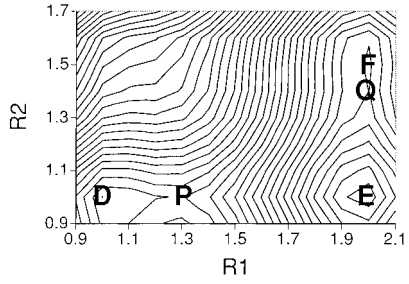


**Figure 9.** The contour plot of the potential energy surface for Case II in the gas phase (HF/6-31G*). Contour lines are plotted at 2.5 kcal/mol intervals.

by adding the relative free energies of solvation to the relative *ab initio* MO energies in gas phase (the HF/6-31G* level). These results are plotted together with the SCRF results. For D → P → E, the calculated free energy of activation by combining *ab initio* MO calculations with Monte Carlo method is 15.5 kcal/mol, 7.5 kcal/mol higher than the SCRF result. On the contrary, for E → Q → F, the calculated free energy of activation is 9.1 kcal/mol, 1.3 kcal/mol lower than the SCRF result.

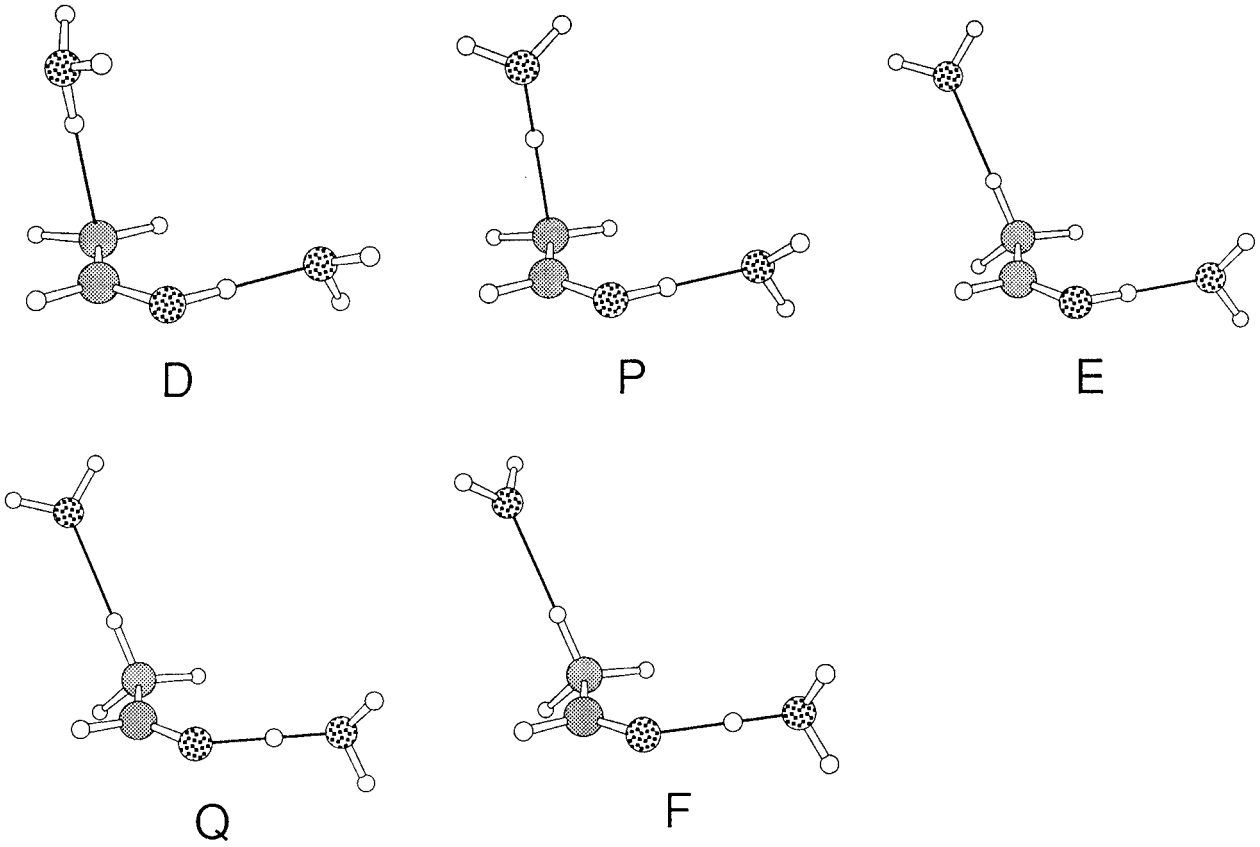


**Figure 10.** The optimized structures for the stationary points, D, P, E, Q, and F, respectively.

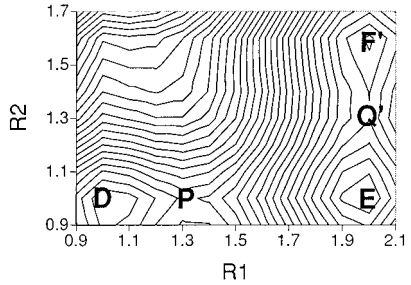


**Figure 11.** The contour plot of the potential energy surface for Case II in the aqueous solution (HF/SCRF/6-31G*). Contour lines are plotted at 2.5 kcal/mol intervals.

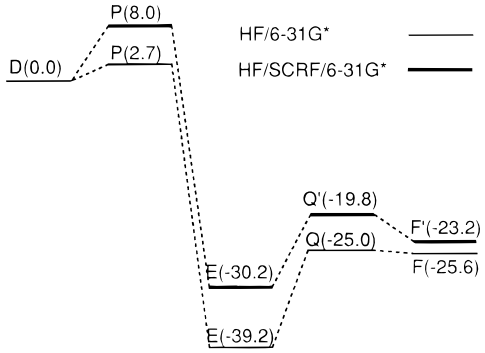


**Figure 12.** Relative energy diagram of Case II with the HF/6-31G* method in the gas phase (HF/6-31G*) and the aqueous solution (HF/SCRF/6-31G*). Numerical values are given in kcal/mol.

**D. Comparison with Experiments.** It is concluded that the cluster study supports almost definitely that the stepwise mechanism, which has been recently suggested by Kresge *et al.*,[7] is more favorable than the concerted one. Moreover, the rate-determining step for the stepwise process has been considered to be the first proton transfer step[2,7] (D → P → E), namely, the proton transfer from hydronium ion to the $\beta$-carbon of VA. Thus, Case II should be naturally preferable to describe the energy profile for the reaction, since, as shown in Figure

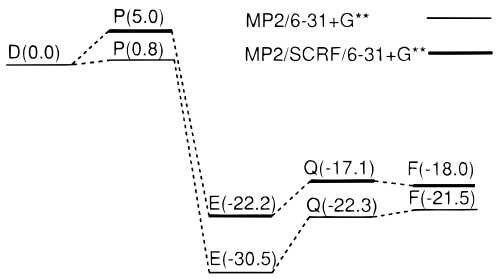


**Figure 13.** Relative energy diagram of Case II with the MP2/6-31+G** method in the gas phase (MP2/6-31+G**) and the aqueous solution (MP2/SCRF/6-31+G**). Numerical values are given in kcal/mol.

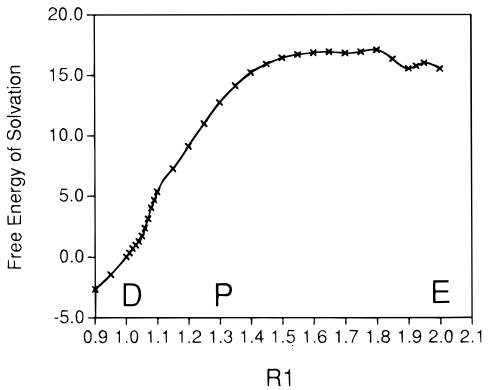


**Figure 14.** Free energy of solvation along the reaction path D → P → E (R1 in angstrom). Numerical values are given in kcal/mol.

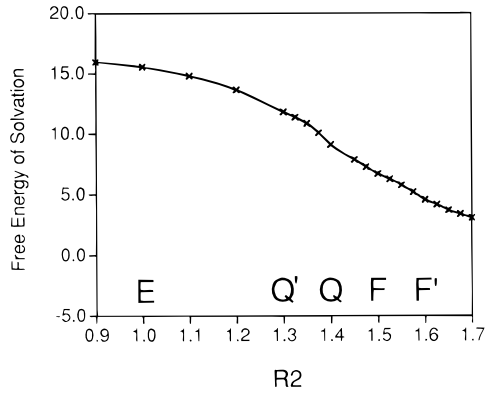


**Figure 15.** Free energy of solvation along the reaction path E → Q(Q′) → F(F′) (R2 in angstroms). Numerical values are given in kcal/mol.

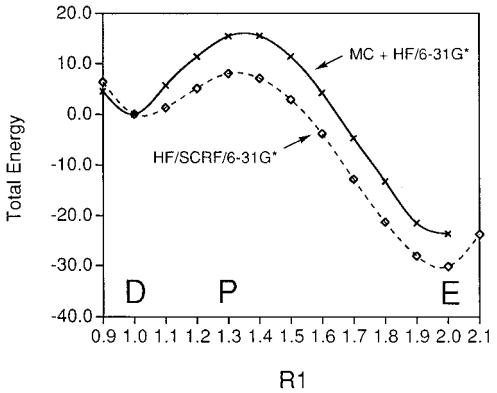


**Figure 16.** The energy profile comparison between MC simulation and the SCRF method along the reaction path D → P → E (R1 in angstroms). Solid line: MC simulations + HF/6-31G* energy. Dashed line: HF/SCRF/6-31G* energy. Numerical values are given in kcal/mol.

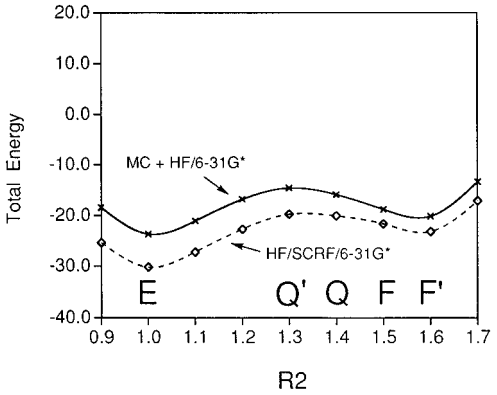


**Figure 17.** The energy profile comparison between MC simulation and the SCRF method along the reaction path E → Q(Q′) → F(F′) (R2 in angstroms). Solid line: MC simulations + HF/6-31G* energy. Dashed line: HF/SCRF/6-31G* energy. Numerical values are given in kcal/mol.

13, the potential energy barrier of the first proton transfer step is 5.0 kcal/mol, while that of the second proton transfer step is 5.1 kcal/mol. However, in Case I, the second transfer step has a potential energy barrier that is quite larger than the first step (Figure 8), indicating that the cluster model for Case I is not suitable for the whole reaction model. From the viewpoint of the dynamics, the first proton transfer completion should induce simultaneously the nuclear reorientation to make the distance *R*(O4−O12) shorter. The selection of 2.60 Å for *R*(O4−O12) (Case II) reflects this synchronized motion (the adiabatic situation).

Monte Carlo simulations executed on the Case II cluster model have reproduced the experimental predictions since the free energy of activation for D → P → E is 15.5 kcal/mol, whereas the free energy of activation for E → Q → F is 9.1 kcal/mol and is smaller than that for the first step, which is in accordance with the experimental suggestion that the first proton transfer step of ketonization is rate-determining. Further, the estimated free energy of activation for the first step is comparable to the experimentally predicted value 15.2 kcal/mol at 25 °C.[6] In addition, consideration of the electron correlation effect has also supported more reliably the fact that the first proton transfer is rate-determining, since, if gas phase MP2 energies are added to the free energies of solvation, the free energy of activation for D → P → E is 13.5 kcal/mol and that for E → Q → F is 1.8 kcal/mol. One might expect simply that the Monte Carlo estimation should reproduce the experimental activation energy much better than the SCRF one. However, it was remarkably unexpected that the second barrier should become quite low and it makes the present reaction resemble apparently the concerted one.

However, in our calculations both with the SCRF method and the Monte Carlo simulations, intermediate B or E is the most stable species during the reaction, whereas Chiang *et al.* estimated that the intermediate is 3.3 kcal/mol higher in free energy than VA.[7] The larger stabilization of the intermediate structures may be exaggeratedly induced by the characteristics of the present cluster models. As shown in Figures 5 and 10, in the structures of A and D, the clusters include a hydronium ion which interacts only with one VA molecule. Therefore, the positive charges in A (or D) can be almost localized at the hydronium ion to make the cluster relatively less stable than B (or E). Similar consideration can be applied to the structure of C and F. However, in the structure of B or E, hydronium ion does not exist and the protonated VA (the intermediate structure) is itself solvated just by two neutral water molecules, leading to the positive charges that can be delocalized to stabilize the whole system. Solvational stabilization taken through the SCRF method and the MC simulations could compensate the above destabilization of A(D) and C(F), and accordingly, the stability of the intermediate structures B and E decreased in effect. However, since the intermediate species are still the most stable, it might be caused by our incomplete treatments. For example, any solvent hydrogen bonding to the cluster was not considered explicitly in the SCRF method and no polarization effect by solvent water molecules was taken into consideration even in the MC simulations.

## IV. Conclusions

*Ab initio* MO calculations combined with the cluster models and the SCRF method revealed that the favorable mechanism for hydronium ion catalyzed isomerization of vinyl alcohol is the stepwise mechanism where the $\beta$-carbon of vinyl alcohol is protonated by hydronium ion in the first step and a proton removal from its hydroxyl group by solvent water occurs at the second step. The calculated potential energy barrier at the MP2/6-31+G** level are 5.0 kcal/mol for the first step and 5.1 kcal/mol for the second step. Although the solvent effect by the SCRF method raises the potential energy barrier of the first step and lowers that of the second step, it is concluded that the present solvent effect is not so large that it changes the whole reaction mechanism within the present SCRF treatment.

On the other hand, Monte Carlo simulations were able to reproduce the experimental free energy change more satisfactorily and revealed clearly that the first proton transfer should

be the rate-determining step. The calculated potential energy barrier is 13.5 kcal/mol for the first step and 1.8 kcal/mol for the second step, which reproduces the realistic circumstances in accordance with experimental prediction that the first step is rate-determining and the energy barrier of activation is 15.2 kcal/mol.

**Acknowledgment.** The authors thank Prof. K. Fukui for his helpful advice and discussion and acknowledge Dr. D. Lim for his kind instruction and advice in the use of ChemEdit and BOSS. The numerical calculations were performed on IBM 355H and NEC SX-4 at the Institute for Fundamental Chemistry and on NEC SX-3 at the Institute for Molecular Science. This work was supported by a Grant-in-Aid for Scientific Research from Ministry of Education, Science and Culture in Japan and partly by the Research for the Future Program of the Japan Society for the Promotion of Science (Project No. JSPS-RFTF96P00206).

JA963994V